

Sum Rate optimization for RIS-Aided RSMA system with Movable Antenna

Mingyu Hu ^{*}, Nan Liu ⁺ and Wei Kang ^{*}

^{*}School of Information Science and Engineering, Southeast University, Nanjing, China 210096

⁺National Mobile Communications Research Laboratory, Southeast University, Nanjing, China 210096
 {myuhu, nanliu, wkang}@seu.edu.cn

Abstract—Rate-Splitting Multiple Access (RSMA) is regarded as a key enabling technique for sixth-generation (6G) wireless systems for its powerful interference management substantially enhancing link throughput. Reconfigurable Intelligent Surface (RIS) can effectively shape the wireless propagation to match the environment and improve communication performance. However, in conventional RSMA–RIS architectures, the antenna elements are fixed, which underutilizes spatial degrees of freedom and hence constrains system performance. To address this limitation, we propose a movable-antenna (MA) assisted RSMA–RIS framework and formulate a sum-rate maximization problem that jointly optimizes the transmit beamforming matrix, the RIS reflection matrix, the common-rate partition, and the MA positions. The original problem is equivalently transformed by employing the fractional programming (FP) method, and a closed-form solution for the common rate splitting is derived. Leveraging the Karush–Kuhn–Tucker (KKT) conditions, we obtain iterative updates for the Lagrange multipliers together with a closed-form expression for the beamforming matrix. We then develop an update rule for the RIS reflection matrix via the dual problem, and finally determine the optimal antenna locations using a gradient-ascent procedure. Numerical results indicate that, even in the presence of RIS assistance, incorporating MAs yields additional performance improvements for RSMA. Moreover, relative to space-division multiple access (SDMA), the assistance of MA yields a greater performance gain for RSMA.

Index Terms—Rate-splitting multiple access (RSMA), reconfigurable intelligent surface (RIS), movable-antenna (MA), Karush–Kuhn–Tucker (KKT) conditions.

I. INTRODUCTION

The concept and basic framework of movable antenna (MA) have been introduced in recent years and have been empirically shown to deliver substantial performance improvements in wireless systems [1]. Compared with conventional fixed-position antenna (FPA), MA connects each radiating element to the radio-frequency (RF) chain via a flexible coaxial cable [2], thereby enabling the element to move within a region spanning several wavelengths. By adaptively repositioning the antenna elements, MA increases spatial degrees of freedom, form high-quality beams, and achieve performance comparable to that of antenna selection (AS) schemes while requiring only a limited number of active elements—thus significantly

This work is partially supported by the National Natural Science Foundation of China under Grants 62361146853, and 62371129, and the Research Fund of the National Mobile Communications Research Laboratory, Southeast University, under Grant 2025A05.

reducing cost. In addition, the inherent flexibility of MA allows free movement in three-dimensional (3D) space, whereas traditional FPAs are typically constrained to one-dimensional (1D) or two-dimensional (2D) layouts, leading to inferior spatial utilization. In recent years, a substantial body of research on MA has emerged. Demonstrated in [3], the deployment of movable antenna (MA) yields significant capacity gains in multiple-input multiple-output (MIMO) systems. The authors of [4] extend the performance enhancement of MA for MIMO systems to the case of statistical channel conditions and derive a closed-form expression for the objective function. Moreover, the performance enhancement of MAs in multiple access channels (MACs) was analyzed in [5], revealing that, compared with conventional uplink systems, the utilization of MAs at user terminals can effectively reduce the overall transmit power consumption. In addition to these studies, MAs have also been empirically verified to improve system performance in various other communication scenarios. For instance, MA can enhance the efficiency of mobile edge computing (MEC) systems [6]. Also, satisfactory secrecy performance can be achieved in covert communication system with the aid of MA even with a limited number of antennas [7]. Furthermore, the authors of [8] investigated MA-assisted reconfigurable intelligent surface–integrated sensing and communication (RIS–ISAC) systems, showing that MAs can reshape the channel characteristics and substantially improve the overall channel gain of ISAC systems.

Rate-Splitting Multiple Access (RSMA) is a multiple-access paradigm poised for next-generation wireless networks. It partitions each user’s message into a common part and a private part, which are encoded into a common stream and private streams, respectively [9]. Users first treat the private streams as noise to decode the common stream and cancel it, thereby partially mitigating multiuser interference followed by which each user treats others’ private streams as noise while decoding its own message. Various RSMA architectures have been developed and studied in which 1-layer RSMA has been demonstrated to deliver strong performance and is widely adopted [10]. Also, RSMA demonstrates robust interference management capabilities under various channel conditions. Specifically, in the limiting cases of weak or strong inter-user interference, it automatically adjusts the split between common and private information and degenerates to

space-division multiple access (SDMA) or non-orthogonal multiple access (NOMA), enabling flexible operation across scenarios [11]. Moreover, RSMA affords higher degrees of freedom than SDMA and NOMA, leading to faster growth of user rates with the signal-to-noise ratio (SNR) [12] [13].

Reconfigurable intelligent surface (RIS) is a kind of meta-surface technology consisting of a two-dimensional array of reflective elements, each of which can independently adjust the phase of the incident signal according to the instantaneous channel, thereby synthesizing highly directive reflected beams and enhancing system performance—especially when the line-of-sight (LoS) path between the base station and users is blocked or severely attenuated by obstacles. Extensive investigations on RIS have been performed across diverse deployment scenarios like in [14] [15] [16].

Typically, RSMA outperforms SDMA and NOMA when practical channels between the base station and users fall between the extremes of orthogonality and full alignment [9]. Since both MA and RIS can actively shape the effective channel, their benefits are expected to be more pronounced for RSMA. To the best of our knowledge, the incremental gains of MAs for RSMA–RIS systems remain unexplored. Motivated by this gap, we propose a downlink multiuser MISO scheme with MA-assisted RSMA–RIS, wherein we maximize the sum rate by jointly optimizing the transmit beamforming matrix, the RIS reflection matrix, the common-rate partition, and the MA positions. The problem is recast via fractional programming (FP) into an equivalent more tractable form. Efficient updates are then derived using the Karush–Kuhn–Tucker (KKT) conditions and associated dual problem. Finally the antenna positions are obtained through a gradient-ascent procedure. Our main contributions are summarized as follows:

- To the best of our knowledge, this is the first work to investigate the incremental benefits of MA for RSMA–RIS systems. We formulate a sum-rate maximization that jointly optimizes the transmit beamforming matrix, the RIS reflection matrix, the common-rate allocation, and the MA positions.
- We propose an alternating optimization (AO) iterative algorithm independent of CVX to solve the formulated optimization problem. Specifically, we derive a closed-form solution for the common-rate allocation and, via FP method, reformulate the original problem into a more tractable equivalent form. Leveraging the KKT condition, we obtain iterative updates for the beamforming matrix. Moreover, we develop an update rule for the RIS reflection matrix through associated dual problem. Finally, gradient-ascent scheme is employed to yield near-optimal MA positions.
- Numerical results show that, even with RIS assistance, incorporating MA further improves RSMA performance. Moreover, the MA-induced improvement for RSMA exceeds that for SDMA, and this advantage becomes more pronounced as the number of users increases.

II. SYSTEM MODEL

In this paper, we consider the system illustrated in Fig. 1, where the base station (BS) is equipped with M movable antennas and employs the 1-layer RSMA scheme to split the user messages. The BS communicates simultaneously with K far-field users with obstacles existing between the BS and the users, causing NLOS path. Each of the antennas can be moved horizontally through flexible cables. Also, a RIS with N reflecting units is placed for the enhancement of the communication performance.

A. Channel Model

In this work, the field response model in [3] is adopted for channel modeling. Denote $\mathcal{M} = \{1, 2, \dots, M\}$ as the set of MA and the positions of them are denoted as a vector $\mathbf{x} = [x_1, x_2, \dots, x_M]$. The end-to-end channel in the system consists of three components. First, we assume that the channel state information (CSI) of the link from the RIS to user k , denoted by $\mathbf{h}_{r,k} \in \mathbb{C}^{N \times 1}$, is available at the base station (BS). Suppose that the signal from BS to RIS will copy L_t versions as transmission and L_r versions as receiver. Then we define the far-field field response vector (FRV) from BS to RIS as:

$$\mathbf{a}(\mathbf{x}_i) = [e^{j \frac{2\pi}{\lambda} \mathbf{x}_i \cos \theta_1^t}, \dots, e^{j \frac{2\pi}{\lambda} \mathbf{x}_i \cos \theta_{L_t}^t}]^T \in \mathbb{C}^{L_t \times 1} \quad (1)$$

where θ_i^t , $i \in \{1, 2, \dots, L_t\}$ denotes the transmit angle corresponding to the i -th propagation path from the BS. Combining all the FRVs, we can obtain the field response matrix (FRM) as:

$$\mathbf{A}(\mathbf{x}) = [\mathbf{a}(\mathbf{x}_1), \mathbf{a}(\mathbf{x}_2), \dots, \mathbf{a}(\mathbf{x}_M)]^T \in \mathbb{C}^{L_t \times M} \quad (2)$$

Similarly, the receive steering vector of the RIS can be defined as:

$$\mathbf{b}_i = [e^{j \frac{2\pi}{\lambda} (x_{r,i} \sin \theta_1^r \cos \phi_1^r + y_{r,i} \cos \theta_1^r)}, \dots, e^{j \frac{2\pi}{\lambda} (x_{r,i} \sin \theta_{L_r}^r \cos \phi_{L_r}^r + y_{r,i} \cos \theta_{L_r}^r)}]^T \in \mathbb{C}^{L_r \times 1} \quad (3)$$

where $(x_{r,i}, y_{r,i})$ is the coordinate of the i -th unit of RIS. θ_i^r and ϕ_i^r respectively denote the elevation and azimuth angles of the i -th propagation path observed at the RIS receiver side. Combining all of these vectors we can get:

$$\mathbf{B} = [\mathbf{b}_1, \mathbf{b}_2, \dots, \mathbf{b}_{N_r}]^T \in \mathbb{C}^{L_r \times N} \quad (4)$$

Then, the equivalent channel matrix between the BS and RIS can be obtained as $\mathbf{H}_{b,r}(\mathbf{x}) = \mathbf{B}^H \Sigma \mathbf{A}(\mathbf{x})$, where Σ is the fading coefficient matrix from the BS to RIS. Likewise, the response matrix corresponding to the BS–user link can be derived as $\mathbf{A}_k(\mathbf{x}) = [\mathbf{a}_k(\mathbf{x}_1), \dots, \mathbf{a}_k(\mathbf{x}_M)]$, where $\mathbf{a}_k(\mathbf{x}_i) = [e^{j \frac{2\pi}{\lambda} \mathbf{x}_i \cos \theta_{k,1}^t}, \dots, e^{j \frac{2\pi}{\lambda} \mathbf{x}_i \cos \theta_{k,L_t}^t}]^T$. The angle $\theta_{k,i}^t$ denotes the transmit angle corresponding to the i -th propagation path from the BS to the k -th user. Then the BS–user channel can be denoted as $\mathbf{h}_{b,k}^H = \mathbf{1}^H \Sigma_k \mathbf{A}_k(\mathbf{x})$. The vector $\mathbf{1}$ is composed entirely of ones and Σ_k is the fading coefficient matrix of BS and the k -th user.

Therefore, the combined equivalent channel matrix from the BS to the k -th user is given by:

$$\mathbf{h}_k^H(\mathbf{x}) = \mathbf{h}_{r,k}^H \Phi \mathbf{H}_{b,r}(\mathbf{x}) + \mathbf{h}_{b,k}^H \quad (5)$$

where $\Phi = \text{diag}([\phi_1, \dots, \phi_N])$ with $|\phi_i| = 1$ the reflection coefficient of the i -th element of RIS.

B. Signal Model

In a 1-layer RSMA, each user message is divided into a common part and a private part. The private part of each user is encoded into $\{s_1, s_2, \dots, s_K\}$. The common parts of each user are combined into one part and consequently encoded into s_c . It is assumed that each stream in $\mathbf{s} = \{s_1, s_2, \dots, s_K, s_c\}$ satisfies $\mathbb{E}[s_i s_i^H] = 1$ and $\mathbb{E}[s_i s_j^H] = 0, \forall i \neq j$. We denote the beamformer of the k -th private stream and common stream as w_k and w_c respectively. Then we can define the beamforming matrix \mathbf{W} as:

$$\mathbf{W} = [\mathbf{w}_1, \dots, \mathbf{w}_K, \mathbf{w}_c] \in \mathbb{C}^{M \times (K+1)} \quad (6)$$

Therefore, the received signal at user k can be expressed as:

$$y_k = \mathbf{h}_k^H \mathbf{W} \mathbf{s} + n_k \quad (7)$$

where $n_k \sim \mathcal{CN}(0, \sigma_k^2)$ is the receive noise of k -th user. According to the 1-layer RSMA scheme, the user decodes the common stream while regarding other streams as interference. After canceling the common part from the stream, users proceed to decode their private parts. The signal-to interference-plus-noise ratio (SINR) for common part at user k can be expressed as:

$$\text{SINR}_{c,k} = \frac{|\mathbf{h}_k^H \mathbf{w}_c|^2}{\sum_{i=1}^K |\mathbf{h}_k^H \mathbf{w}_c|^2 + \sigma_k^2} \quad (8)$$

Consequently, we can get the common rate for the k th user:

$$R_{c,k} = \log(1 + \text{SINR}_{c,k}) \quad (9)$$

The private SINR at the k th user is given by

$$\text{SINR}_k = \frac{|\mathbf{h}_k^H \mathbf{w}_k|^2}{\sum_{i=1, i \neq k}^K |\mathbf{h}_k^H \mathbf{w}_i|^2 + \sigma_k^2} \quad (10)$$

The private rate for the k th user is:

$$R_k = \log(1 + \text{SINR}_k) \quad (11)$$

C. Problem Formulation

To investigate whether MA can further enhance system performance when the RIS is already deployed to improve communication, we formulate an optimization problem that aims to maximize the sum of both the private and common

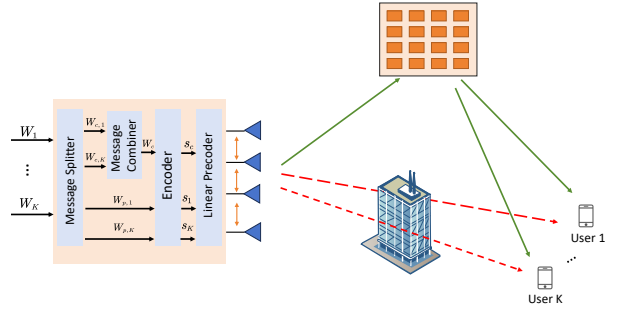


Fig. 1. System model of an MA-aided RSMA-RIS system.

achievable rates of all users. The optimization problem is formulated as:

$$(\mathbf{P1}) \max_{\mathbf{x}, \mathbf{W}, \Phi, \{r_{c,k}\}} R = \sum_{k=1}^K (R_k + r_{c,k}) \quad (12a)$$

$$\text{s.t. } \text{tr}(\mathbf{W}^H \mathbf{W}) \leq P_T, \quad (12b)$$

$$\sum_{k=1}^K r_{c,k} \leq R_{c,k}, \quad \forall k, \quad (12c)$$

$$r_{c,k} \geq 0, \quad \forall k, \quad (12d)$$

$$|\phi_i| = 1, \quad \forall i \in \mathcal{M}, \quad (12e)$$

$$X_{min} \leq \mathbf{x}_i \leq X_{max} \quad (12f)$$

$$\|\mathbf{x}_i - \mathbf{x}_j\|_2 \geq D_0, \quad \forall i \neq j. \quad (12g)$$

where P_T is the power budget of the BS, and $\{r_{c,k}\}$ is the common rate allocated to the k th user. D_0 is the minimum inter-antenna spacing between any two antennas. X_{min} and X_{max} are the limits of region for MA. (12b) is the power constraint. (12c) is the common rate constraint to make sure that every user can successfully encode the common symbol. (12d) represents the non-negativity constraint of the common rate. (12e) represents the constant-modulus constraint imposed on each RIS element. (12f) represents the minimum inter-antenna spacing constraint.

Due to the non-convex nature of (12a), (12e), and (12g), as well as the strong coupling among the optimization variables, problem (P1) is evidently a highly non-convex optimization problem. In the subsequent sections, we develop an efficient alternating optimization (AO) optimization algorithm to solve this problem.

III. PROPOSED SOLUTION

In this section, we propose an efficient AO algorithm to solve problem (P1). Specifically, by fixing a subset of variables and optimizing the remaining ones, the original problem is decomposed into several tractable subproblems. Moreover, closed-form solutions are derived in the optimization process, which eliminates the need for standard optimization solvers such as CVX and significantly reduces the overall computational complexity.

A. Updating allocating common rates

When all optimization variables except for the allocated common rate are fixed, the original problem can be transformed into:

$$\max_{\{r_{c,k}\}} \sum_{k=1}^K r_{c,k} \quad (13a)$$

$$\text{s.t. } \sum_{k=1}^K r_{c,k} \leq R_{c,k}, \quad \forall k, \quad (13b)$$

$$r_{c,k} \geq 0, \quad \forall k. \quad (13c)$$

Constraint (13b) can be equivalently transformed into $\sum_{k=1}^K r_{c,k} \leq \min\{R_{c,k}\}, \forall k$. It is evident that the objective function achieves its maximum value when this constraint holds with equality. Therefore, we can set $r_{c,k}^* = \frac{1}{K} \min\{R_{c,k}\}$.

B. Updating other variables by FP

In this section, the FP method [17] is employed to transform the intractable non-convex objective function and constraints (12c) into a more tractable form. By substituting the optimal common rate into (P1) and applying the FP-based reformulation, an equivalent problem, denoted as (P2), can be obtained as:

$$(\mathbf{P2}) \max_{\mathbf{W}, \Phi, \mathbf{x}, \mu, \epsilon, \gamma, \mathbf{v}, y} \sum_{k=1}^K \Psi_k(\mu, \epsilon, \mathbf{W}, \mathbf{x}, \Phi) + y \quad (14a)$$

$$\text{s.t. } \text{tr}(\mathbf{W}^H \mathbf{W}) \leq P_T, \quad (14b)$$

$$T_k(\mu, \mathbf{v}, \mathbf{W}, \Phi, \mathbf{x}) \geq y, \quad \forall k, \quad (14c)$$

$$|\phi_i| = 1, \quad \forall i \in \mathcal{M}, \quad (14d)$$

$$X_{\min} \leq x_i \leq X_{\max}, \quad \forall i \in \mathcal{M}, \quad (14e)$$

$$\|\mathbf{x}_i - \mathbf{x}_j\|_2 \geq D_0, \quad \forall i \neq j. \quad (14f)$$

where y is an auxiliary variable, and μ, ϵ, γ , and \mathbf{v} are auxiliary variables introduced by the FP technique. The functions Ψ_k and T_k are given in (15) and (16).

1) *Updating Auxiliary Variables $\mu, \gamma, \epsilon, \mathbf{v}$:* It is noteworthy that when other variables are fixed, equations (15) and (16) are concave functions with respect to the auxiliary variables. Consequently, their updates can be obtained by taking the corresponding derivatives. However, it should be emphasized that the derivations of μ and γ are computed with respect to the Lagrangian-transformed functions prior to the FP reformulation [17], whereas the remaining two auxiliary variables are directly differentiated from equations (15) and (16). The updates of auxiliary variables are given as:

$$\mu_k^* = \frac{|\mathbf{h}_k^H \mathbf{w}_k|^2}{\sum_{i \neq k}^K |\mathbf{h}_k^H \mathbf{w}_i|^2 + \sigma_k^2} \quad (17)$$

$$\epsilon_k^* = \frac{\sqrt{1 + \mu_k} \mathbf{h}_k^H \mathbf{w}_k}{\sum_{i=1}^K |\mathbf{h}_k^H \mathbf{w}_i|^2 + \sigma_k^2} \quad (18)$$

$$\gamma_k^* = \frac{|\mathbf{h}_k^H \mathbf{w}_c|^2}{\sum_{i=1}^K |\mathbf{h}_k^H \mathbf{w}_i|^2 + \sigma_k^2} \quad (19)$$

$$v_k^* = \frac{\sqrt{1 + \gamma_k} \mathbf{h}_k^H \mathbf{w}_c}{|\mathbf{h}_k^H \mathbf{w}_c|^2 + \sum_{i=1}^K |\mathbf{h}_k^H \mathbf{w}_i|^2 + \sigma_k^2} \quad (20)$$

2) *Updating beamforming matrix \mathbf{W} and auxiliary variable y :* The original problem (P2) can be reformulated as:

$$(\mathbf{P2.1}) \max_{\mathbf{W}, y} \sum_{k=1}^K \Psi_k(\mathbf{W}) + y \quad (21a)$$

$$\text{s.t. } T_k(\mathbf{W}) \geq y, \quad \forall k, \quad (21b)$$

$$\text{tr}(\mathbf{W}^H \mathbf{W}) \leq P_T. \quad (21c)$$

(P2.1) is obviously convex so that some useful tools can be used to solve it like CVX. While in this subsection, we will develop an efficient algorithm for solving the beamforming matrix by exploiting the KKT conditions. The Lagrangian function of problem (P2.1) is given by:

$$\mathcal{L}(\mathbf{W}, \{\lambda_k\}, \kappa) = \sum_{k=1}^K \Psi_k(\mathbf{W}) - y + \sum_{k=1}^K \lambda_k(y - T_k(\mathbf{W})) + \kappa(\text{tr}(\mathbf{W}^H \mathbf{W}) - P_T) \quad (22)$$

where $\{\lambda_k\}$ and κ are the Lagrange multipliers associated with constraints (21b) and (21c), respectively. Furthermore, the KKT conditions can be derived as followed:

$$\mathbf{w}_c^* = \left(\sum_{k=1}^K \lambda_k^* |\mathbf{v}_k|^2 \mathbf{h}_k \mathbf{h}_k^H + \kappa^* \mathbf{I} \right)^{-1} \left(\sum_{k=1}^K \lambda_k^* \sqrt{1 + \gamma_k} \mathbf{v}_k \mathbf{h}_k \right), \quad (23a)$$

$$\mathbf{w}_m^* = \left(\sum_{k=1}^K (|\epsilon_k|^2 + \lambda_k^* |\mathbf{v}_k|^2) \mathbf{h}_k \mathbf{h}_k^H + \kappa^* \mathbf{I} \right)^{-1} \sqrt{1 + \mu_m} \epsilon_m \mathbf{h}_m, \quad (23b)$$

$$\sum_{k=1}^K \lambda_k^* = 1, \quad (23c)$$

$$\lambda_k^*(y^* - T_k(\mathbf{W}^*)) = 0, \quad \forall k, \quad (23d)$$

$$\kappa^*(\text{tr}(\mathbf{W}^{*H} \mathbf{W}^*) - P_T) = 0, \quad (23e)$$

$$\lambda_k^* \geq 0, \quad \kappa^* \geq 0. \quad (23f)$$

Among them, equations (23a)~(23c) arise from stationarity condition, while equations (23d) and (23e) correspond to

$$\Psi_k(\cdot) = \log(1 + \mu_k) - \mu_k + \underbrace{2\sqrt{1 + \mu_k} \Re\{\epsilon_k^H \mathbf{h}_k^H \mathbf{w}_k\}}_{\Psi_{k,1}} - \underbrace{|\epsilon_k|^2 \left(\sum_{i=1}^K |\mathbf{h}_k^H \mathbf{w}_i|^2 + \sigma_k^2 \right)}_{\Psi_{k,2}} \quad (15)$$

$$T_k(\cdot) = \log(1 + \gamma_k) - \gamma_k + 2\sqrt{1 + \gamma_k} \Re\{\mathbf{v}_k^H \mathbf{h}_k^H \mathbf{w}_c\} - |\mathbf{v}_k|^2 \left(|\mathbf{h}_k^H \mathbf{w}_c|^2 + \sum_{i=1}^K |\mathbf{h}_k^H \mathbf{w}_i|^2 + \sigma_k^2 \right) \quad (16)$$

the complementary slackness conditions. According to the structure of problem (P2.1), the optimal value of y is

$$y^* = T_w(\mathbf{W}). \quad (24)$$

where w denotes the user index corresponding to the minimum value of T_k . By combining (23d), (23e), (24) and applying the fixed point iteration method in [18], the update rules for the Lagrange multipliers can be derived as follows:

$$\lambda_k^{[t+1]} = \frac{T_w(\mathbf{W}) + \rho}{T_k(\mathbf{W}) + \rho} \lambda_k^{[t]}, \quad k \neq w, \quad (25a)$$

$$\lambda_w^{[t+1]} = \lambda_w^{[t]} + \sum_{k=1}^K \left(\lambda_k^{[t]} - \frac{T_w(\mathbf{W}) + \rho}{T_k(\mathbf{W}) + \rho} \lambda_k^{[t]} \right), \quad (25b)$$

$$\kappa^{[t+1]} = \frac{\text{tr}(\mathbf{W} \mathbf{W}^H) + \rho}{P_T + \rho}. \quad (25c)$$

where constant $\rho \geq 0$ is employed to enhance convergence stability by effectively reducing the step size. Equation (25b) is designed to ensure that the KKT condition (23c) is satisfied during iteration.

3) *Updating RIS reflection matrix Φ :* In this subsection, we present a low-complexity iterative algorithm for updating the RIS reflection matrix. The equivalent channel matrix from the base station to user k can be simplified as $\mathbf{h}_k^H = \phi^H \mathbf{U}_k + \mathbf{u}_k^H$, where $\phi = \text{diag}(\Phi^H)$, $\mathbf{U}_k = \text{diag}(\mathbf{h}_{r,k}^H) \mathbf{B}^H \mathbf{\Sigma} \mathbf{A}$, $\mathbf{u}_k = \mathbf{A}_k^H \mathbf{\Sigma}_k \mathbf{1}$. By substituting the simplified channel vector into problem (P2) and fixing the other variables, we obtain:

$$(\mathbf{P2.2}) \max_{\phi} -\phi^H \mathbf{M}_1 \phi + \Re\{\phi^H (\mathbf{M}_2 - 2\mathbf{M}_3)\}, \quad (26a)$$

$$\text{s.t. } |\phi_i|^2 = 1, \quad \forall i, \quad (26b)$$

$$\begin{aligned} \sum_{k=1}^K r_{c,k} &\leq -\phi^H \mathbf{N}_{1,k} \phi \\ &+ \Re\{\phi^H (\mathbf{N}_{2,k} - \mathbf{N}_{3,k})\} + d, \quad \forall k. \end{aligned} \quad (26c)$$

where $\mathbf{M}_1 = \mathbf{U}_k (\sum_{k=1}^K |\epsilon_k|^2 \sum_{i=1}^K \mathbf{w}_i \mathbf{w}_i^H) \mathbf{U}_k^H$, $\mathbf{M}_2 = \sum_{k=1}^K 2\sqrt{1 + \mu_k} \epsilon_k^H \mathbf{U}_k \mathbf{w}_k$, $\mathbf{M}_3 = \mathbf{U}_k (\sum_{k=1}^K |\epsilon_k|^2 \sum_{i=1}^K \mathbf{w}_i \mathbf{w}_i^H) \mathbf{u}_k$, $\mathbf{N}_{1,k} = |\mathbf{v}_k|^2 \mathbf{U}_k (\mathbf{w}_c \mathbf{w}_c^H + \sum_{i=1}^K \mathbf{w}_i \mathbf{w}_i^H) \mathbf{U}_k^H$, $\mathbf{N}_{2,k} = 2\sqrt{1 + \mu_k} \mathbf{v}_k^H \mathbf{U}_k \mathbf{w}_c$, $\mathbf{N}_{3,k} = 2|\mathbf{v}_k|^2 \mathbf{U}_k (\mathbf{w}_c \mathbf{w}_c^H - \sum_{i=1}^K \mathbf{w}_i \mathbf{w}_i^H) \mathbf{u}_k$, $d = 2\sqrt{1 + \gamma_k} \Re\{\mathbf{v}_k^H \mathbf{u}_k^H \mathbf{w}_c\} |\mathbf{v}_k|^2 \mathbf{u}_k^H (\mathbf{w}_c \mathbf{w}_c^H + \sum_{i=1}^K \mathbf{w}_i \mathbf{w}_i^H) \mathbf{u}_k$. The dual problem of (P2.2) is given by:

$$\max_{\xi} \min_{\phi} \mathcal{L}(\phi, \xi) \quad (27a)$$

$$\text{s.t. } |\phi_i|^2 = 1, \quad \forall i \in \{1, \dots, N\}. \quad (27b)$$

where $\mathcal{L}(\phi, \xi) = \phi^H \mathbf{M}_1 \phi - \Re\{\phi^H (\mathbf{M}_2 - 2\mathbf{M}_3)\} + \sum_{i=1}^K \xi_i (\sum_{k=1}^K r_{c,k} + \phi^H \mathbf{N}_{1,i} \phi - \Re\{\phi^H (\mathbf{N}_{2,i} - \mathbf{N}_{3,i})\} - d)$, $\xi = [\xi_1, \xi_2, \dots, \xi_K]^T$ denotes the lagrangian multiplier. we employ the dual ascent method to solve this problem. First, the Lagrange multipliers are fixed to update ϕ . After some algebraic manipulations, we obtain $\mathcal{L}(\phi, \xi) = \phi^H (\mathbf{M}_1 + \sum_{i=1}^K \xi_i \mathbf{N}_{1,i}) \phi - \Re\{\phi^H (\mathbf{M}_2 - 2\mathbf{M}_3 + \sum_{i=1}^K \xi_i (\mathbf{N}_{2,i} - \mathbf{N}_{3,i}))\} + \sum_{i=1}^K \xi_i (\sum_{k=1}^K r_{c,k} - d)$. Combining with (27b) and $\phi^H (\mathbf{M}_1 + \sum_{i=1}^K \xi_i \mathbf{N}_{1,i}) \phi \leq \phi^H \lambda_{\max} \mathbf{I} \phi + 2\Re\{\phi^H (\mathbf{M}_1 + \sum_{i=1}^K \xi_i (\mathbf{N}_{1,i} - \lambda_{\max} \mathbf{I})) \phi^t\}$, where ϕ^t denotes the optimal value of ϕ obtained in the previous iteration and λ_{\max} is the maximum eigenvalue of matrix $\mathbf{M}_1 + \sum_{i=1}^K \xi_i \mathbf{N}_{1,i}$, we can get the upper bound of the lagrangian function as:

$$\mathcal{L}(\phi, \xi) \leq \Re\{\phi^H \mathbf{h}\} \quad (28)$$

where $\mathbf{h} = 2(\mathbf{M}_1 + \sum_{i=1}^K \xi_i \mathbf{N}_{1,i} - \lambda_{\max} \mathbf{I}) \phi^t - (\mathbf{M}_2 - 2\mathbf{M}_3 + \sum_{i=1}^K \xi_i (\mathbf{N}_{2,i} - \mathbf{N}_{3,i}))$. Therefore, the optimal solution of ϕ is given by:

$$\phi^{[t+1]} = e^{j \angle \mathbf{h}} \quad (29)$$

In addition, the gradient ascent method is employed to update ξ . Specifically, the gradient $\nabla_{\xi} \mathcal{L}(\phi^t, \xi)$ is selected as the update direction of ξ . In summary, the iterative update formulas for ξ and ϕ are given as follows:

$$\begin{aligned} \xi_i^{[t+1]} &= \left[\xi_i^{[t]} + \left(\sum_{k=1}^K r_{c,k} + \phi^H \mathbf{N}_{1,i} \phi \right. \right. \\ &\quad \left. \left. - \Re\{\phi^H (\mathbf{N}_{2,i} - \mathbf{N}_{3,i})\} - d \right) \tau \right]^+, \quad \forall i \end{aligned} \quad (30a)$$

$$\Phi^{[t+1]} = \text{diag}(e^{j \mathbf{h}}). \quad (30b)$$

where τ is the step size for gradient ascent and can be set to a small fixed value. $[\cdot]^+ = \max\{0, \cdot\}$ is the projection function for the Lagrange multiplier ξ .

$$\nabla_{\mathbf{x}_m} \Psi_1(\mathbf{x}) = 2 \sum_{k=1}^K \sum_{m'=1}^{L_t} \sum_{m=1}^M \sqrt{1 + \mu_k} \left(-\frac{2\pi}{\lambda} \cos \theta_{k,m'} \right) |\epsilon_k \mathbf{a}_{m'}(\mathbf{w}_k)_m| \sin \left(\frac{2\pi}{\lambda} \cos \theta_{k,m'} \right) \angle \left(\epsilon_k^* \mathbf{a}_{m'}^*(\mathbf{w}_k)_m \right) \\ - \frac{2\pi}{\lambda} \cos \theta_{k,m'} |\epsilon_k \mathbf{a}_{m'}(\mathbf{w}_k)_m| \sin \left(\frac{2\pi}{\lambda} \cos \theta_{k,m'} \right) \quad (31)$$

4) *Updating MA positions*: With other parameters fixed, we can get the subproblem as follows:

$$(\mathbf{P2.3}) \max_{\mathbf{x}} \Psi(\mathbf{x}) = \sum_{k=1}^K \Psi_k(\mathbf{x}) \quad (32a)$$

$$\text{s.t. } T_k(\mathbf{x}) \geq y, \forall k \quad (32b)$$

$$(14e), (14f) \quad (32c)$$

Considering the non-convex nature of this problem, we employ the gradient ascent method to update the position of the MA. The gradient of the objective function with respect to \mathbf{x}_m is denoted as $\nabla_{\mathbf{x}_m} \Psi(\mathbf{x})$. Accordingly, the position of the MA is updated as follows:

$$\mathbf{x}_m^{(t+1)} = \mathbf{x}_m^{(t)} + \alpha (\nabla_{\mathbf{x}_m} \Psi_1(\mathbf{x}) + \nabla_{\mathbf{x}_m} \Psi_2(\mathbf{x})), \quad (33)$$

where $\Psi_1(\mathbf{x}) = \sum_{k=1}^K \Psi_{k,1}(\mathbf{x})$ and $\Psi_2(\mathbf{x}) = \sum_{k=1}^K \Psi_{k,2}(\mathbf{x})$. α denotes the step size of the gradient ascent iteration. Even if a feasible initial solution is selected, the gradient ascent procedure may still violate the feasible region during the iteration process. In such cases, the step size α is reduced to 0.5α to ensure that the updated position remains within the feasible set R_f , where R_f is the feasible region for problem (P2.3). The gradient of $\Psi_1(\mathbf{x})$ can be calculated by (31), where $\mathbf{a}^H = \mathbf{h}_{r,k}^H \Phi \mathbf{B}^H, \mathbf{b}^H = \mathbf{1}^H \Sigma^k$, and $(\cdot)_m$ represents the m^{th} element of vector (\cdot) . The gradient $\nabla_{\mathbf{x}_m} \Psi_2(\mathbf{x})$ exhibits a similar structure and is omitted for brevity. The overall algorithm for solving problem (P1) is displayed in **Algorithm 2**.

C. Complexity Analysis

The computational complexity of **Algorithm 1** is approximately $\mathcal{O}(N_G M^2 K^2 L_t^2)$, where N_G denotes the total number of iterations in the gradient ascent procedure. In **Algorithm 2**, the complexities of updating the FP parameters and the Lagrange multipliers are $\mathcal{O}(8M)$ and $\mathcal{O}(2M(K+1) + K)$, respectively. During the beamforming matrix update, the matrix inversion step significantly increases the computational cost. To mitigate this, LU decomposition can be employed to reduce the inversion complexity in which case only one LU factorization is required, and the subsequent inverse computations incur a complexity of $\mathcal{O}(M^2)$. In summary, assuming that the total number of outer iterations is N_T , the overall computational complexity of the proposed algorithm can be approximately expressed as $\mathcal{O}(M^3 + N_T(8M + 2M(K+1) + K + M^2 + N_G M^2 K^2 L_t^2))$.

IV. NUMERICAL RESULTS

In this paper, we assume that the number of multipath components is $L_t = L_r = 4$, and that the elevation and

Algorithm 1 Gradient Descent for Solving Problem (P2.3)

- 1: **Initialization:** Initialize $\mathbf{x}^{(l)} \in \mathcal{R}_f$. Set iteration index $l = 0$, objective value $\Psi^{(l)} = 0$, and threshold $\epsilon > 0$.
- 2: Compute $\Psi^{(l+1)}$.
- 3: **repeat**
- 4: Update $\mathbf{x}^{(l+1)}$ by (32).
- 5: **if** $\mathbf{x}^{(l+1)} \notin \mathcal{R}_f$ **then**
- 6: $\alpha = 0.5\alpha$.
- 7: **else**
- 8: $\Psi^{(l)} = \Psi^{(l+1)}$.
- 9: $l = l + 1$.
- 10: Compute $\Psi^{(l+1)}$.
- 11: **end if**
- 12: **until** $|\Psi^{(l+1)} - \Psi^{(l)}| \leq \epsilon$ or $l \geq l_{\max}$
- 13: **Output:** $\mathbf{x}^{(l+1)}$.

Algorithm 2 AO for Solving Problem (P1)

- 1: **Initialization:** Set $\{\lambda^r, \kappa^r, \mu^r, \epsilon^r, \mathbf{v}^r, \gamma^r, \mathbf{W}^r, \mathbf{x}^r, \Phi^r, \xi^r, r_{c,k}^r, R^r, R^{r+1}, R_{c,k}^r, T_k^r, T_k^{r+1}\}$. Set iteration index $r = 0$, maximum iteration number r_{\max} , and threshold ϵ .
- 2: **repeat**
- 3: $R^r = R^{r+1}, T_k^r = T_k^{r+1}, \forall k$.
- 4: Update $\mu^{r+1}, \epsilon^{r+1}, \mathbf{v}^{r+1}, \gamma^{r+1}$ by (17)–(20).
- 5: Update $\lambda^{r+1}, \kappa^{r+1}$ by (25a)–(25c).
- 6: Update \mathbf{W}^{r+1} by (23a) and (23b).
- 7: Calculate $R_{c,k}^{r+1}$ and update $r_{c,k}^{r+1}$ by $r_{c,k}^{r+1} = \frac{1}{K} \min_{\forall k} \{R_{c,k}^{r+1}\}$.
- 8: Update ξ^{r+1} and Φ^{r+1} by (30a) and (30b).
- 9: Update \mathbf{x}^{r+1} by **Algorithm 1**.
- 10: Calculate R^{r+1}, T_k^{r+1} and set $r = r + 1$.
- 11: **until** $|R^{r+1} - R^r| < \epsilon$ or $r \geq r_{\max}$
- 12: **Output:** R^{r+1} .

azimuth angles of all propagation paths are uniformly distributed within the range $[0, \pi]$. Except for Fig. 3, the number of communication users is set to $K = 2$, the number of BS antennas is $M = 8$, and the number of reflecting elements on the RIS is $N = 16$. The carrier frequency is assumed to be $f = 2.4 \times 10^9$ Hz, yielding a wavelength of $\lambda = \frac{c}{f}$, where c denotes the speed of light. The movable antenna elements are allowed to move within the range of $[-6\lambda, 6\lambda]$, and the minimum spacing between adjacent antennas is set to half a wavelength. The noise power is assumed to be -80 dBm. Furthermore, the BS is located at the coordinate origin, while the RIS is positioned at (12 m, 16 m). The user

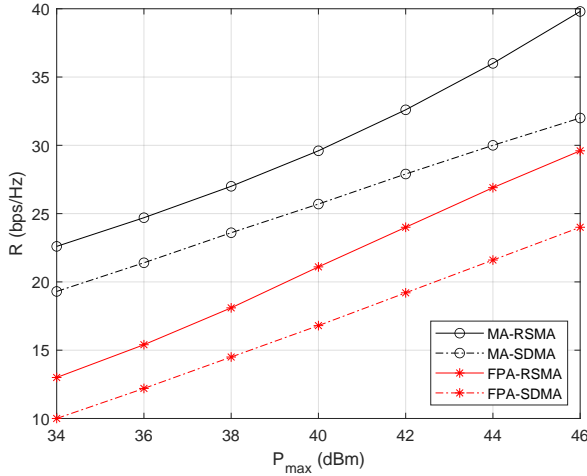


Fig. 2. Power budget versus sum rate

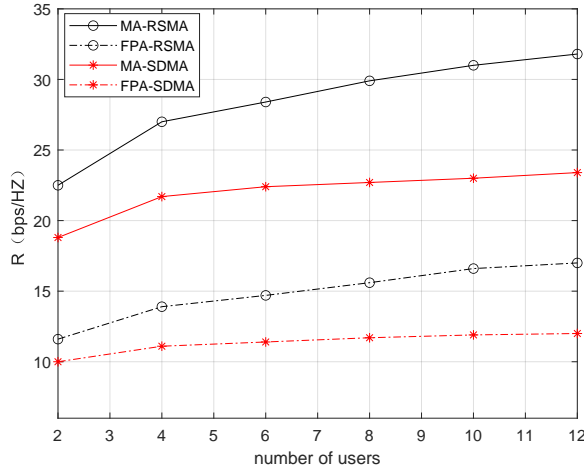


Fig. 3. Number of users versus sum rate

terminals are uniformly distributed within a rectangular area defined by $[20 \text{ m}, 40 \text{ m}] \times [0 \text{ m}, -20 \text{ m}]$. It is assumed that there is no LOS path between the BS and CU, owing to the presence of multiple obstacles, whereas LoS links exist for both the BS–RIS and RIS–CU channels. Consequently, the diagonal elements of the BS–CU channel fading matrix Σ_k is modeled as $\Sigma_k[i, i] \sim \mathcal{CN}\left(0, \frac{1}{p+1} C_0 \left(\frac{d_0}{d}\right)^{\alpha_1} / L\right)$, where $C_0 = \left(\frac{\lambda}{4\pi}\right)^2$. For the BS–IRS channel Σ , the diagonal elements of the fading matrices are respectively given by $\Sigma[1, 1] \sim \mathcal{CN}\left(0, \frac{p}{p+1} C_0 \left(\frac{d_0}{d}\right)^{\alpha_c}\right)$ and $\Sigma[i, i] \sim \mathcal{CN}\left(0, \frac{1}{p+1} C_0 \left(\frac{d_0}{d}\right)^{\alpha_c} / (L-1)\right)$, where p is the Rician factor set as 0.5, $c \in \{2, 3\}$ denotes the indices corresponding to the BS–IRS and IRS–CU links respectively. The path-loss exponents for the three channels are set as $\alpha_1 = 3.5$, $\alpha_2 = 2.5$, and $\alpha_3 = 2.5$.

First, we investigate how the sum rate R scales with the maximum transmit power P_{\max} in Fig. 2. As expected, R increases monotonically with P_{\max} , and the slope for RSMA

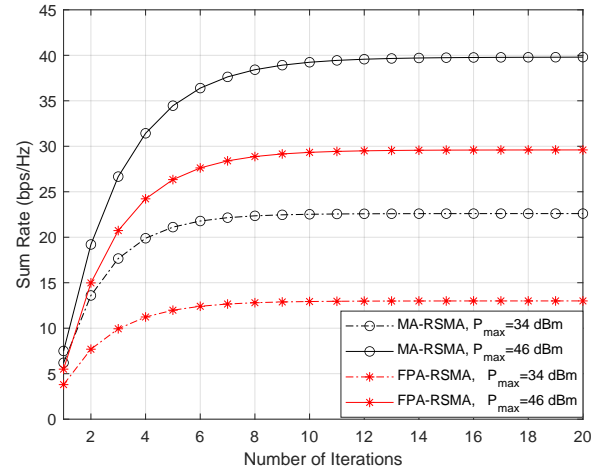


Fig. 4. Iteration number versus sum rate

is larger than that for SDMA, which is because RSMA affords higher degrees of freedom (DoF) than SDMA. Furthermore, it can be observed that both SDMA-RIS and RSMA-RIS systems achieve significant performance gains with the incorporation of MA. However, the improvement is more pronounced for the RSMA system. Specifically, MA provides approximately a 34.4% performance enhancement for the RSMA system, compared to about 32.3% for the SDMA system, indicating that MAs shape the channel in a manner more favorable to RSMA.

In Fig. 3, we examine the relationship between the number of users K and the sum rate. Overall, the sum rate increases with K , but the increments diminish as K becomes larger. Moreover, the MA-assisted RSMA–RIS curve exhibits a steeper slope than the alternatives, indicating that the MA-induced improvement is more pronounced for RSMA than for SDMA as K grows. Specifically, when the number of users reaches 12, the MA yields a gain of approximately 15.2 bps/Hz for the RSMA system, whereas it provides only 11.7 bps/Hz for the SDMA system. Moreover, as observed from the figure, this performance gap continues to widen with the increasing number of users. Intuitively, when K increases, MA must reshape the user channels toward near-orthogonality to substantially benefit SDMA, whereas RSMA does not require such stringent orthogonality to achieve strong performance.

Finally, Fig. 4 analyzes the evolution of the RSMA sum rate versus the iteration index under two transmit-power constraints. Across all four schemes, the curves converge in approximately ten iterations and then remain stable, with the higher-power setting reaching a larger steady-state sum rate.

V. CONCLUSION

In this work, we investigate a MA assisted RSMA–RIS downlink MISO system and maximize the sum rate via joint optimization of the transmit beamforming matrix, the common-rate allocation, the RIS reflection matrix, and the

MA positions. We develop an efficient solution based on a FP reformulation to solve this problem. Numerical results demonstrate that, relative to SDMA, MA assistance delivers a more pronounced improvement in the sum-rate performance of RSMA–RIS.

REFERENCES

- [1] L. Zhu, W. Ma, and R. Zhang, “Modeling and performance analysis for movable antenna enabled wireless communications,” *IEEE Transactions on Wireless Communications*, vol. 23, no. 6, pp. 6234–6250, 2023.
- [2] S. Nithya, T. Jagadesh, E. Shalini, T. Sathiyapriya, V. Teresa, and P. R. Buvaneswari, “Design and development of movable antenna system for multiplatform wireless communication,” in *2022 IEEE 2nd Mysore Sub Section International Conference (MysuruCon)*. IEEE, 2022, pp. 1–5.
- [3] W. Ma, L. Zhu, and R. Zhang, “Mimo capacity characterization for movable antenna systems,” *IEEE Transactions on Wireless Communications*, vol. 23, no. 4, pp. 3392–3407, 2023.
- [4] G. Yan, L. Zhu, and R. Zhang, “Movable antenna aided multiuser communications: Antenna position optimization based on statistical channel information,” *arXiv preprint arXiv:2502.20856*, 2025.
- [5] L. Zhu, W. Ma, B. Ning, and R. Zhang, “Movable-antenna enhanced multiuser communication via antenna position optimization,” *IEEE Transactions on Wireless Communications*, vol. 23, no. 7, pp. 7214–7229, 2023.
- [6] Y. Cang, M. Chen, and Z. Yang, “Movable antenna enhanced mec systems with discrete antenna position selection,” *IEEE Communications Letters*, 2025.
- [7] P. Liu, J. Si, Z. Cheng, Z. Li, and H. Hu, “Movable-antenna enabled covert communication,” *IEEE Wireless Communications Letters*, 2024.
- [8] H. Wu, H. Ren, C. Pan, and Y. Zhang, “Movable antenna-enabled ris-aided integrated sensing and communication,” *IEEE Transactions on Cognitive Communications and Networking*, 2025.
- [9] Y. Mao, B. Clerckx, and V. O. Li, “Rate-splitting multiple access for downlink communication systems: Bridging, generalizing, and outperforming sdma and noma,” *EURASIP journal on wireless communications and networking*, vol. 2018, no. 1, p. 133, 2018.
- [10] C. Hao, Y. Wu, and B. Clerckx, “Rate analysis of two-receiver miso broadcast channel with finite rate feedback: A rate-splitting approach,” *IEEE Transactions on Communications*, vol. 63, no. 9, pp. 3232–3246, 2015.
- [11] Y. Mao, O. Dizdar, B. Clerckx, R. Schober, P. Popovski, and H. V. Poor, “Rate-splitting multiple access: Fundamentals, survey, and future research trends,” *IEEE communications surveys & tutorials*, vol. 24, no. 4, pp. 2073–2126, 2022.
- [12] C. Hao, B. Rassouli, and B. Clerckx, “Achievable dof regions of mimo networks with imperfect csit,” *IEEE Transactions on Information Theory*, vol. 63, no. 10, pp. 6587–6606, 2017.
- [13] E. Piovano and B. Clerckx, “Optimal dof region of the k -user miso bc with partial csit,” *IEEE Communications Letters*, vol. 21, no. 11, pp. 2368–2371, 2017.
- [14] Q. Wu and R. Zhang, “Intelligent reflecting surface enhanced wireless network via joint active and passive beamforming,” *IEEE transactions on wireless communications*, vol. 18, no. 11, pp. 5394–5409, 2019.
- [15] C. Huang, A. Zappone, G. C. Alexandropoulos, M. Debbah, and C. Yuen, “Reconfigurable intelligent surfaces for energy efficiency in wireless communication,” *IEEE transactions on wireless communications*, vol. 18, no. 8, pp. 4157–4170, 2019.
- [16] Z. Yang, M. Chen, W. Saad, W. Xu, M. Shikh-Bahaei, H. V. Poor, and S. Cui, “Energy-efficient wireless communications with distributed reconfigurable intelligent surfaces,” *IEEE Transactions on Wireless Communications*, vol. 21, no. 1, pp. 665–679, 2021.
- [17] K. Shen and W. Yu, “Fractional programming for communication systems—part i: Power control and beamforming,” *IEEE Transactions on Signal Processing*, vol. 66, no. 10, pp. 2616–2630, 2018.
- [18] T. Fang and Y. Mao, “Rate splitting multiple access: Optimal beamforming structure and efficient optimization algorithms,” *IEEE Transactions on Wireless Communications*, 2024.